



Isocyanate-free tannin-based polyurethane resins for enhancing thermo-mechanical properties of ramie (*Boehmeria nivea* L.) fibers

Muhammad Adly Rahandi Lubis^{a,b}, Manggar Arum Aristri^{a,c}, Rita Kartika Sari^c,
Apri Heri Iswanto^{d,*}, Syeed Saifulazry Osman Al-Edrus^e, Jajang Sutiawan^{a,d}, Seng Hua Lee^f,
Petar Antov^g, Lubos Kristak^h

^a Research Center for Biomass and Bioproducts, National Research and Innovation Agency, Cibinong 16911, Indonesia

^b Research Collaboration Center for Biomass and Biorefinery, BRIN and Universitas Padjadjaran, Jatinangor 40600, Indonesia

^c Department of Forest Products, Faculty of Forestry and Environment, IPB University, Bogor 16680, Indonesia

^d Department of Forest Product, Faculty of Forestry, Universitas Sumatera Utara, Padang Bulan, Medan 20155, Indonesia

^e Institute of Tropical Forestry and Forest Products, Universiti Putra Malaysia, UPM, Serdang 43400, Selangor, Malaysia

^f Department of Wood Industry, Faculty of Applied Sciences, Universiti Teknologi MARA (UiTM), Kampus Jengka, Bandar Tun Razak 26400, Pahang, Malaysia

^g Faculty of Forest Industry, University of Forestry, 1797 Sofia, Bulgaria

^h Faculty of Wood Sciences and Technology, Technical University in Zvolen, 96001 Zvolen, Slovakia

ARTICLE INFO

Keywords:

Acacia mangium bark
Bio-NIPU resin
Dimethyl carbonate
Hexamethylenediamine
Impregnation

ABSTRACT

The objective of this research was to investigate and evaluate the possibility of increasing the thermo-mechanical properties of ramie (*Boehmeria nivea* L.) fibers by impregnating them with a tannin-based non-isocyanate polyurethane (Bio-NIPU) resin. The resin was created by reacting tannin of *Acacia mangium* with dimethyl carbonate (DMC) and hexamethylenediamine (HMDA). The optimal time of impregnation was discovered to be 90 min, as demonstrated by its thermal stability, with a residual of 25% remaining after being treated to a temperature of 750 °C. When ramie fibers were impregnated with the newly developed tannin-based Bio-NIPU resin, their thermal and mechanical qualities significantly enhanced. In terms of mechanical properties, the impregnated ramie fibers had a tensile strength of 325 MPa and an elasticity modulus of 10.82 GPa. Py-GCMS was used to confirm the production of urethane groups as a result of the reaction between the tannin-based Bio-NIPU resin and ramie fibers. The use of FE-SEM in conjunction with EDS allowed the detection of nitrogen from urethane groups in Bio-NIPU. The characterization analysis also demonstrated that incorporating tannin-based Bio-NIPU resin into ramie fibers had a substantial impact on their thermal and mechanical properties, increasing their potential for wider use across varied industrial sectors.

1. Introduction

Polyurethane (PU) is a polymer containing the urethane functional group. PU is commercially manufactured using polycondensation processes involving diisocyanates and diols (polyols) obtained from petroleum refining [1]. Due to the growing demand for PU production associated with unsustainable consumption of fossil resources, more ecologically friendly renewable materials are required. Renewable polyols derived from plant feedstocks, including tannins, can be used to obtain PU [2]. Conversely, the issue of toxicity associated with isocyanates presents a significant obstacle that necessitates the undertaking of extensive research in this domain. Non-isocyanate polyurethanes

(NIPU) can be synthesized by combining diols/polyols with carbonates, which are subsequently reacted with amines, resulting in a production of NIPU resins [3–6].

Tannins are natural polyphenolic compounds which can be derived from a variety of plants, including *Acacia mangium*. Tannins can be categorised into two distinct groups: hydrolysable tannins, encompassing gallotannins and ellagitannins, and condensed polyflavonoid tannins. The worldwide production of tannins achieved a significant milestone in 2020, totaling 1.3 million tonnes [7]. According to data from the Ministry of Environment and Forestry, roundwood production in Indonesia until November 2023 is 53.96 million m³. This figure is lower than roundwood production in 2022, which will reach 64.65

* Corresponding author.

E-mail address: apri@usu.ac.id (A.H. Iswanto).

<https://doi.org/10.1016/j.aej.2024.01.044>

Received 9 October 2023; Received in revised form 28 December 2023; Accepted 13 January 2024

Available online 30 January 2024

1110-0168/© 2024 The Author(s). Published by Elsevier BV on behalf of Faculty of Engineering, Alexandria University This is an open access article under the CC BY-NC-ND license (<http://creativecommons.org/licenses/by-nc-nd/4.0/>).

million m³ and in 2021 that approximately reach 55.55 million m³. The decline in roundwood production in Indonesia may be caused by various factors, such as weather conditions, market demand, government policies and environmental issues. The most widely produced type of wood in Indonesia in 2022 is acacia, with a volume of 31.54 million m³ or 48.79% of the total national roundwood production. Acacia wood is widely used for the paper, pulp and plywood industries [8]. The mangium tree is composed of approximately 30–50% wood and 10.5–12.1% bark [9]. In addition, significant quantities of mangium bark are available as by-products of the pulp and paper industry, and most of them are still underutilized in non-value-added applications, e.g. for production of energy. Markedly, mangium bark is characterized by a relatively high tannin content, estimated to 33.63% [10,11].

In the framework of synthesising tannin-based NIPU resins, it is plausible for two distinct reactions involving tannin, dimethyl carbonate (DMC), and hexamethylene diamine (HMDA). The reaction between HMDA and a carboxyl group is facilitated by the interaction between the hydroxyl group of tannin and DMC [12]. The reaction is commonly referred to as a "carbonate formation" reaction. Following the carbonate production process, the tannin undergoes modification, resulting in the incorporation of carbonate groups. Subsequently, carbonated tannin can react with HMDA. The HMDA amino groups react with the carbonate groups on the tannin, resulting in the creation of urethane bonds. Most tannin-based NIPU resins are utilized as wood adhesives [3,13].

The textile industry generally focuses on aesthetics, design, and comfort of the garments. In contrast, the development of technical textiles prioritizes their use functions such as technical properties, performance, and utilization for non-decorative purposes. Usually, industrial development in this field aims to combine several physical properties and enable its use in specific environments and conditions [14]. The use of these technical textiles is very diverse. They can be categorized as sports textiles, which can be used as materials to support sports activities such as flying, gliding, rowing, and climbing. In addition, there are also transport textiles where the fabric is usually reinforced or coated to improve physical properties and facilitate use under pressure [15]. Other examples include medical textiles (fabrics must have antibacterial properties and certain chemical resistance) and industrial and protective clothing, which should enhance workers' protection against harmful and hazardous working conditions, e.g. be resistant to heat, fire, radiation, and chemicals, or provide better visibility [16]. Occupational health and safety issues in the industrial world are of primary importance, so it is necessary to develop technical textiles with relevant characteristics, minimizing workers' exposure to hazards, and thus preventing that workplace injuries and diseases [17]. Therefore, this study aimed to synthesize tannin-based NIPU resins for the modification of ramie fiber by impregnation to improve the fiber's thermal and mechanical performance.

2. Experimental

2.1. Materials

The equipment utilised in this study consisted of a pH meter (Horiba, LAQUA F72, Kyoto, Japan), a rotary evaporator (B-300 BÜCHI Labor-technik AG, Flawil, Switzerland), a hotplate stirrer (IKA C-MAG HS 7, IKA-Werke GmbH & Co. KG, Staufen, Germany), a 1 L vacuum chamber (VC0918SS, VacuumChambers.ue, Białystok, Poland), an analytical balance (Pioneer PX224, OHAUS, Parsippany, NJ, USA), a Dynamic Mechanical Analyser (DMA 8000, PerkinElmer, MA, USA), a thermogravimetric analyzer TGA4000 (Perkin Elmer, MA, USA), Py-GCMS (Shimadzu Corporation, Kyoto, Japan), and a field emission scanning electron microscope (FE-SEM, Quattro S, Thermo Fisher Scientific Inc., Waltham, MA, USA) coupled with EDX (Ultim Max, Oxford UK).

The study utilised mangium bark (*Acacia mangium*) sourced from PT. TELPP (Palembang, Indonesia) and ramie fiber obtained from CV. Rabersa (Wonosobo, Indonesia). The additional components employed

in the experiment consisted of distilled water, dimethyl carbonate (DMC 99%, SigmaAldrich, Hamburg, Germany), and hexamethylene diamine (HMDA 99%, SigmaAldrich, Hamburg, Germany).

2.2. Methods

2.2.1. Tannin extraction process

The extraction of tannin from Mangium bark (40–60 mesh) was conducted using the maceration method, employing a hot water (w/v) ratio of 1:10. The mixture was thereafter heated to a temperature of 60 °C and subjected to stirring using a magnetic stirrer for a duration of 6 h. The filtrate was acquired subsequent to the filtration of the extract. The extraction process was iterated four times until the filtrate achieved clarity. In addition, the liquid that passed through the filter was subjected to evaporation using a rotary evaporator under specific conditions of 60 °C temperature and 22 mBar pressure, resulting in the production of a concentrated tannin extract. Fig. 1 illustrates the flow chart depicting the process of tannin extraction.

2.2.2. Tannin-based NIPU resin synthesis process

A tannin-based NIPU was synthesized by reacting tannin extract with DMC in a 1:1 ratio at a temperature of 50 ± 2 °C, followed by stirring for a duration of 15 min. Subsequently, the sample was supplemented with HMDA at a tannin-to-HMDA ratio of 4:1. The resulting mixture was then subjected to stirring at a speed of 500 rpm for a duration of 30 min (Fig. 2).

2.2.3. Ramie fiber impregnation

The degummed ramie fibers were impregnated with tannin Bio-NIPU resin using a vacuum pump (VacuumChambers.ue, Białystok, Poland). A total of 3 g of ramie fibers were immersed in a solution containing 30 mL of tannin Bio-NIPU resin. The impregnation process took place at a controlled temperature of 27 ± 2 °C, at a pressure of 50 kPa, and lasted for a duration of 1 h. Subsequently, the fibers that had been impregnated were subjected to a drying process at a temperature of approximately 25 ± 2 °C under normal atmospheric conditions for a duration of 24 h. The weight gain of dried ramie fibers was assessed through measurement following the impregnation process.

2.2.4. Characterization of tannin, tannin-based NIPU resins, and ramie fiber

2.2.4.1. Thermal stability. The thermal stability of tannin, tannin Bio-NIPU, and ramie fiber before and after impregnation were examined by the utilization of the TGA instrument. A quantity of 20 mg of material was measured and subjected to heating within a nitrogen atmosphere, utilizing a flow rate of 20 mL/min., in a Standard Ceramic Crucible. The heating temperature spanned from 25 to 750 °C, with a heating rate of 10 °C/min. The Pyris 11 Software (Version 11.1.1.0492, Pyris, MA, USA) was employed for the computation of the percentage weight loss, weight loss rate, and residue.

2.2.4.2. Thermo-mechanical properties. The samples of viscous tannin and tannin Bio-NIPU resin were individually impregnated on filter paper. Thermo-mechanical analyses were conducted using a Dynamic Mechanical Analyzer (DMA 8000, PerkinElmer, MA, USA) in dual cantilever mode, with a constant frequency of 1 Hz. The temperature range for the analysis was set between 20–50 °C. The viscoelastic behaviour was characterized by determining the storage modulus (E'), loss modulus (E''), and damping factor (tan δ) of each sample at heating rates of 2 °C/min. The graphs were displayed using Pyris 11 program.

The ramie fiber samples, before and after impregnation, were impregnated to a filter paper (CAT No.1005–125, Whatman, UK). Thermal and mechanical evaluations were conducted on filter paper impregnated with viscous tannin extract. These evaluations were

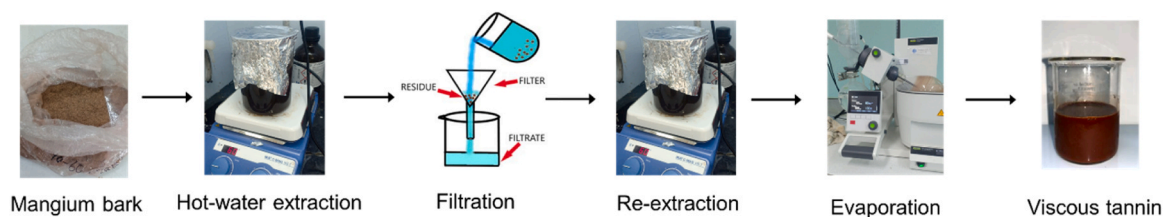


Fig. 1. Flow chart of tannin extraction using hot-water.

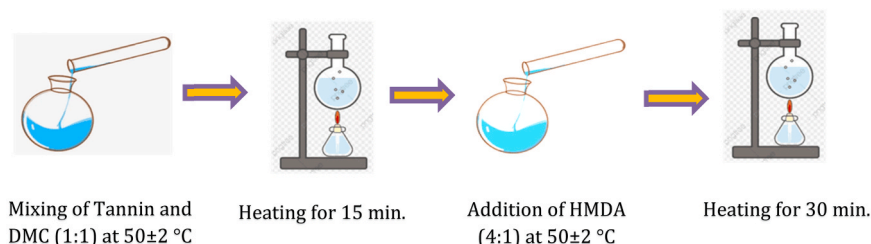


Fig. 2. Illustration of tannin-based NIPU synthesis.

performed utilizing a dual cantilever mode DMA with a constant frequency drag of 1 Hz, throughout a temperature range of 20–50 °C. The viscoelastic behaviour of the samples was characterized by determining the storage modulus (E'), loss modulus (E''), and $\tan \delta$ through a heating process at average rates of 2 °C/min. Subsequently, the Pyris 11 program was employed to present the graphical representations.

2.2.4.3. Py-GCMS analysis of tannin extract and tannin-based NIPU resins. Samples of tannin extract, tannin Bio-NIPU, and ramie fibers each weighing 500–600 μg , were introduced into the ecocup (SF PYI-EC50F). Subsequently, the cup was sealed with glass wool, and the samples were subjected to evaluation using the Pyrolysis–Gas Chromatography–Mass Spectrometry (Py-GCMS) equipment (Shimadzu, Kyoto, Japan). The eco-cup underwent pyrolysis at a temperature of 500 °C for a duration of 0.1 min using a multi-shot pyrolysis system (EGA/PY-3030D) connected to a QP-2020 NX GC/MS system (Shimadzu, Kyoto, Japan). The GC/MS system was equipped with an SH-Rxi-5Sil MS column, which had a film thickness of 30 μm , an inner diameter of 0.25 mm, and a particle size of 0.25 μm . The system operated with 70 eV electrons and helium as the carrier gas. The recorded atmospheric pressure was measured at 20.0 kilopascals (15.9 mL/min.), with a column flow rate of 0.61 mL/min.). The temperature profile for GC involved an initial temperature of 50 °C for a duration of 1 min. Subsequently, the temperature was increased to 280 °C at a heating rate of 5 °C/min. Following this, the temperature was maintained at 280 °C for a period of 13 min. The identification of pyrolysis products in the 2017 NIST LIBRARY project was achieved by the comparison of retention time and mass spectrum data.

2.2.5. Morphological and mechanical testing of modified ramie fiber

2.2.5.1. Morphological and chemical properties of ramie fibers. The morphological and chemical characteristics of ramie fibers were examined by the utilization of FE-SEM & EDX at a magnification of 1000x, employing a power of 3.0 kV and $\text{K}\alpha 1$ X-ray.

2.2.5.2. Mechanical properties of modified ramie fiber. The evaluation of the tensile strength and modulus of elasticity of modified ramie fibers was conducted according to the ASTM D 3379–75 standard, utilizing a universal testing machine (UTM, AGX, Shimadzu, Kyoto, Japan) [8]. The specimens included in the study consisted of individual fibers that were isolated from strand bonds. The length of the specimens ranged between 20 and 30 mm, whereas the entire length of the fibers was

estimated to be nearly three times that of the specimens. The specimens underwent testing with a loading force of 5000 N and a crosshead speed of 1 mm/min. The experiments were conducted at a controlled ambient temperature of 25 ± 2 °C.

3. Result and discussions

3.1. Thermal properties of tannin and tannin-based NIPU resins

The thermal stability of tannin and tannin-based NIPU resins was examined using the TGA-DTG (Fig. 3). This study elucidates the correlation between alterations in bulk or degradation of tannin and tannin-based NIPU resins as a function of temperature. The weight loss seen in both samples initially took place at temperatures below 100 °C, resulting from the evaporation of water and tannin components [18]. The weight loss of the tannin Bio-NIPU resin at a temperature of 100 °C exhibited a higher magnitude compared to the weight loss observed in extract tannins, which was measured at a rate of 0.4% per degree Celsius. The weight loss seen at temperatures ranging from – 220 to + 220 degrees Celsius was around 0.4% per degree Celsius, suggesting a breakdown of the carbohydrate bonds present in tannins. According to Wang et al. tannin aromatic bonds undergo further oxidative degradation at a temperature of approximately 450 °C, resulting in a significant

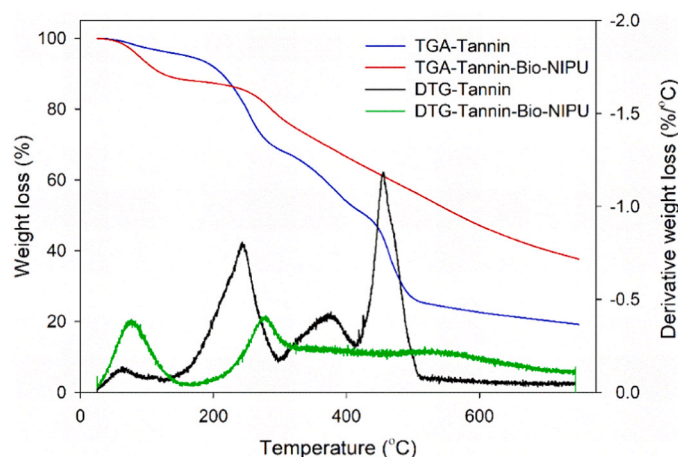


Fig. 3. TGA-DTG thermograms of tannin and tannin-Bio-NIPU resins.

weight loss of approximately 1.25%/°C [19]. The thermal breakdown of aromatic tannin rings and the principal oxidative mechanism of tannins have been observed to take place at temperatures over 450 °C, as reported by Chattopadhyay and Webster [20], Handika et al. [21] and Wang et al. [19]. The residual weight of tannin exhibited a variability of $\pm 21\%$, whereas a weight loss of around 79% was observed. The 21% is the amount of residue or remaining charcoal produced at the end of the heating process, and the amount of weight loss that occurs is 79% of the initial weight when the sample was tested by TGA. Due to the intricate aromatic tannin structures and potential for cross-linking that can occur during synthesis, tannin can serve as a viable substitute for polyols in the production of NIPU resins designed for high-temperature applications.

The resin decomposes in two phases: the initial phase is the evaporation of water process, and the second one, more important phase is the resin decomposition phase. The resin loses 10% of its weight at 109.88 °C, that was could be related to the reduction in moisture absorbed or the appearance of water evaporate processes but does not include degradation of the resin its structure [22]. A weight loss of 25% occurred at 311.57 °C due to the decomposition process of the urethane bonds and the chemicals compound, that they were not strongly bonded at the time of the polymerization process [23]. In contrast, at 562.24 °C a further oxidative breakdown of the resin was observed, resulting in a 50% weight reduction. The primary oxidative tannin reactions, the disintegration of aromatic tannin rings, and the deterioration of the polymer's three-dimensional structure occur above 450 °C [21]. The stability of the tannins obtained in this work was lower when compared to tannin Bio-NIPU at the end of the decomposition process at a

temperature of 744.43 °C with a residue level of 37.61%. This might be because the tannin extract contains more carbohydrates overall, primarily from the sugar in the final tannin structure. In addition, compared to the tannin extract before it was synthesized into resin, the tannin Bio-NIPU resin formed a urethane structure, increasing its stability [24].

3.2. Viscoelastic and thermo-mechanical properties

The DMA testing is employed to ascertain the viscoelastic and thermomechanical characteristics of a polymer, specifically in relation to its molecular structure. The findings of the thermomechanical investigation conducted on tannins and tannin Bio-NIPU resins are depicted in Fig. 4. The resulting thermomechanical properties yield three types of information: storage modulus (E'), loss modulus (E''), and damping factor ($\tan \delta$). These properties are influenced by temperature and frequency and can be utilised to elucidate the interfacial bonding of the composite material [25,26]. The value of E' and E'' of the two samples were determined by analysing their response to increasing temperatures and the glass transition temperature (T_g), which can be identified by the peak of the $\tan \delta$ curve. The findings shown in Fig. 4 indicate that the value of E' of tannin was lower (± 495 GPa) compared to the E' value obtained from tannin Bio-NIPU resin (± 528 GPa). In Fig. 4a, there is a noticeable decline in the value of E' for tannins until it reaches a temperature of approximately ± 38 °C, at which point it reaches a minimum value of ± 459 GPa. Subsequently, there is an increase in E' to approximately ± 462 GPa.

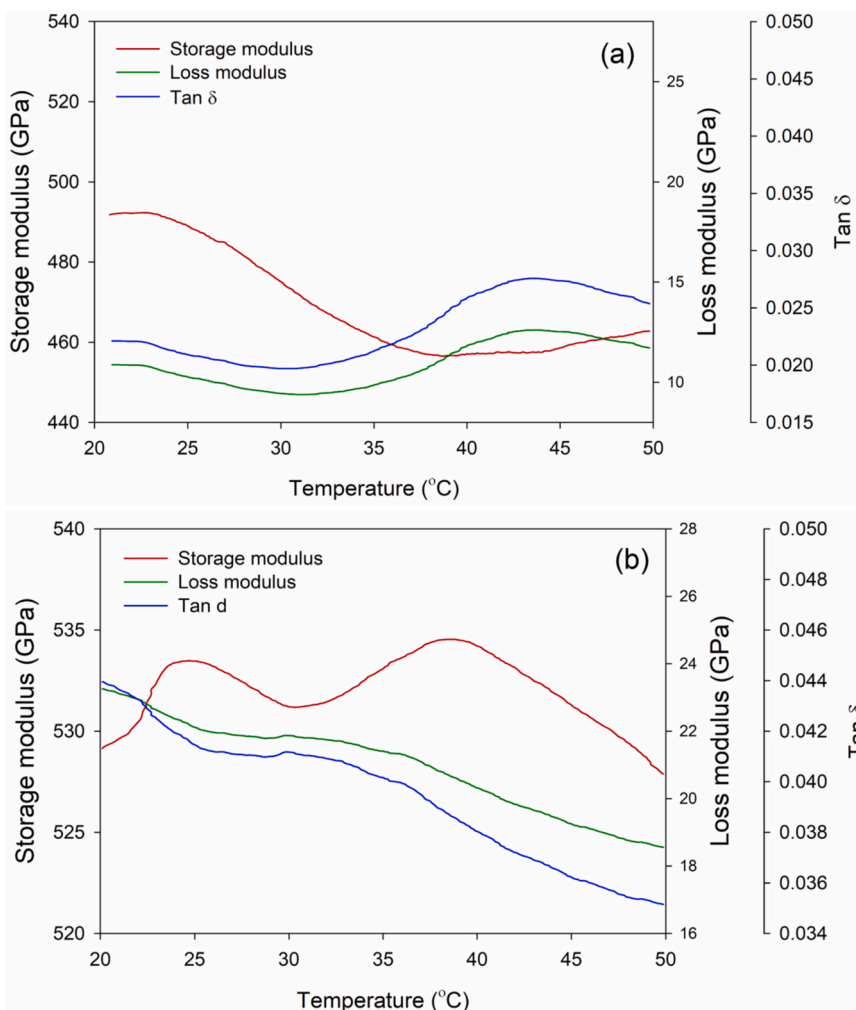


Fig. 4. DMA thermograms of tannin-Bio-NIPU resins: (a) Tannin (b) Tannin Bio-NIPU.

Conversely, Fig. 4b illustrates the variable nature of E' yield for Bio-NIPU throughout the temperature range of ± 20 – 40 °C. At a temperature of 40 °C, the tannin Bio-NIPU exhibited the maximum E' of 534 GPa, followed by a decrease to 529 GPa. The relationship between the enhanced rigidity and stiffness of a material and the corresponding elevation in the value of E' is observed, hence influencing the material's elastic response and its capacity to sustain the provided energy. A high value of E' indicates the occurrence of the hardening process within the sample. According to the data presented in Fig. 4, it can be observed that the tannin Bio-NIPU resin exhibited a higher E' value in comparison to tannin alone. The occurrence of this phenomenon can be attributed to the polymerization technique employed in the manufacturing of tannic Bio-NIPU resin. The elevated E' value can be attributed to the increased strength and stiffness of the bonds created within the material, resulting in enhanced resistance to the displacement of molecular chains. Consequently, a greater amount of energy is required to bring these chains into proximity with chain segments [27].

The influence of viscosity on the material's behaviour can be characterised by two key parameters: the loss modulus (E'') and the damping factor ($\tan \delta$). These parameters are indicative of the internal energy dissipation resulting from various factors such as plastic deformation, friction within the material, molecular motion, relaxation processes, phase transitions, and morphological changes [28]. The E'' of tannins exhibited a similar pattern to that of E' , wherein it fell as the temperature climbed, and afterwards saw a notable increase after reaching a temperature of approximately ± 33 °C. In contrast, it was observed that the tannin resin content in Bio-NIPU exhibited a downward trend with increasing temperature.

The initial E' value of tannins, measured at a temperature of 20 °C, was around 11 GPa, with an uncertainty of measurement. Subsequently, this value reduced to 5 GPa within the temperature range of 20 – 31 °C. The loss modulus value of tannins reached its maximum at temperatures of ± 43 °C, with a corresponding value of ± 13 GPa. The acquired results exhibit a direct proportionality to the previously determined values of storage modulus. Nevertheless, the rise in the loss modulus value observed beyond 40 °C remained comparatively lower than the increase in the storage modulus. This implies that a greater amount of energy is required to induce a change in the shape of the tannins and for elastically recoverable deformation. The E' for the resin material was measured to be ± 23.8 GPa at a temperature of 20 °C. Subsequently, the modulus reduced to ± 18.2 GPa when the temperature was raised to 50 °C. Nevertheless, the loss modulus value shown a decrease, albeit being greater in comparison to tannins. The dissipation of energy resulting from irreversible viscous deformation, which arises from the alteration of a material's shape under specific pressure and temperature conditions, can also serve as a means to ascertain the viscosity of that substance. The T_g can be determined by identifying the temperature at which the loss modulus curve reaches its peak, as suggested by Wang et al. [29]. This approach is commonly employed to evaluate the low-temperature characteristics of materials [29].

At an initial temperature ranging from 20 to 50 °C, the $\tan \delta$ value of the tannin Bio-NIPU resin was observed to be greater (Fig. 4b) compared to that of tannin alone (Fig. 4a). Specifically, the $\tan \delta$ values for the resin ranged from 0.035 to 0.043 , while for tannin they ranged from 0.021 to 0.025 . The loss modulus proportion and the material's capacity for irreversible deformation have a positive correlation with higher $\tan \delta$ values. The observed elevation in the aforementioned value can be attributed to an augmentation in the interplay between hydroxyl groups (polyphenols) derived from tannins and DMC and HMDA substances, ultimately leading to polymerization processes and consequent amplification of the E'' to E' ratio. According to Menczel and Prime [30], a decrease in deformation energy results in a reduction of viscous dissipation as heat. The increase in the resin's $\tan \delta$ value is attributed to internal friction and viscoelastic energy dissipation, which are known to intensify at elevated temperatures. This phenomenon indicates that higher rigidity of the polymer molecule leads to reduced molecular

mobility, thereby enhancing the interfacial bonding between polymer chains beyond the level observed in tannin [28].

3.3. Py-GC-MS analysis of tannin and tannin-based NIPU resin

Based on the results of an analysis using Py-GC-MS instrument (Fig. 5a), it can be seen that at a retention time of 1.93 min, tannins showed a peak of the carbon dioxide component with the highest relative abundance (%), and the result is 82.49% . Basak et al. [31] demonstrated that tannins at high temperatures release carbon dioxide and benzene triol. The outer gallic acid layer of the tannin structure is decarboxylated to produce benzene triol [31]. In Fig. 5, it is confirmed that in the retention time of 20.67 min, there is a chemical component in form of 1-benzofuran-5-ol. Based on the findings of the tannin TGA-DTG curve (Fig. 3), this phenomenon is also strengthened, which shows a degradation peak at temperatures above 220 °C and 750 °C tannin still has a residue of around 21% which confirms that the ester linkage that exists between the benzene's rings in the outer and inner layers has undergone a cleavage process and the inner gallic acid layer's decarboxylation to produce a chemical component in the form of carbon dioxide which is not flammable.

In addition, there is a possibility that the breaking of the ester bond causes the gallic acid layer of the inner tannin to also experience cross-linking (aromatization or dehydration) with benzene diol on the outer layer, which results in the tannin having a residue of more than 35% charcoal even though it has been heated at 500 °C. In addition to the high carbon dioxide content, the retention time of 20.144 min also indicated the presence of a resorcinol chemical component in tannins of 14.23% . Resorcinol is a component of the tannin flavonoid unit. Ismayati et al. (2016) stated that resorcinol has a chemical component as a fraction of the A-ring pyrolysis product in tannins [32]. Based on the results of the pyrogram, it can also be seen that the type of tannin used is hydrolyzed tannin because carbon dioxide was found as a result of the pyrolysis fraction of gallic acid, where the gallic acid is a fraction of galotannin monomer (one type of hydrolyzed tannin monomer) which is easily cut apart, unlike condensed tannins which are not easily cut off. In addition, there are several component fractions resulting from tannin pyrolysis products with a relatively small abundance in tannins, such as nickel tetracarbonyl (0.87% and 0.22%), acetone (0.77), 2-(Phenylmethyl)phenol, trimethylsilyl ether (0.18%), and 2-Methyl-5-hydroxy benzofuran (0.48%).

Fig. 5a also shows the results of pyrolysis of resin. The tannin Bio-NIPU resin underwent a pyrolysis process and was degraded into specific molecular fractions, such as retention times of $13,055$ and $14,891$ min which indicated the presence of the 1,6-Hexanediamine fraction with a relative abundance of 21.13% and 1,2-Ethanediamine, respectively. N-ethyl-N'-methyl (0.35%) derived from the hexamethylenediamine molecule used in the tannin synthesis of Bio-NIPU resin. In addition, at a retention time of 6.922 , it showed the presence of the Azocine fraction, octahydro- with a relative abundance of 0.55% which results from the degradation of urethane polymers and includes cyclic ciano groups. The results of polyurethane degradation are also shown from the relative abundance (70.62%) at retention time $34,904$ which is a molecular fraction of 5-Amivaleric acid, N-methoxycarbonyl-, methyl ester and 1-Pentanamine, N,N-dimethyl- with a relative abundance of 0.34% at a retention time of 26.11 , and the molecular fraction of carbonated tannins and tannins Bio-NIPU resin showed a retention time of 25.173 and an abundance of 6.26% namely N-(Ethoxycarbonyl)hexamethylenediamine. In addition, the degradation of polyurethane was also confirmed by the presence of cyclic amide groups in the form of the caprolactam fraction at a retention time of 18.32 of 0.76% . As a complement, Fig. 5b shows the scheme reaction of tannin Bio-NIPU.

3.4. Thermal properties of ramie fibers

Based on the analysis of the TGA-DTG results shown in Fig. 6, the

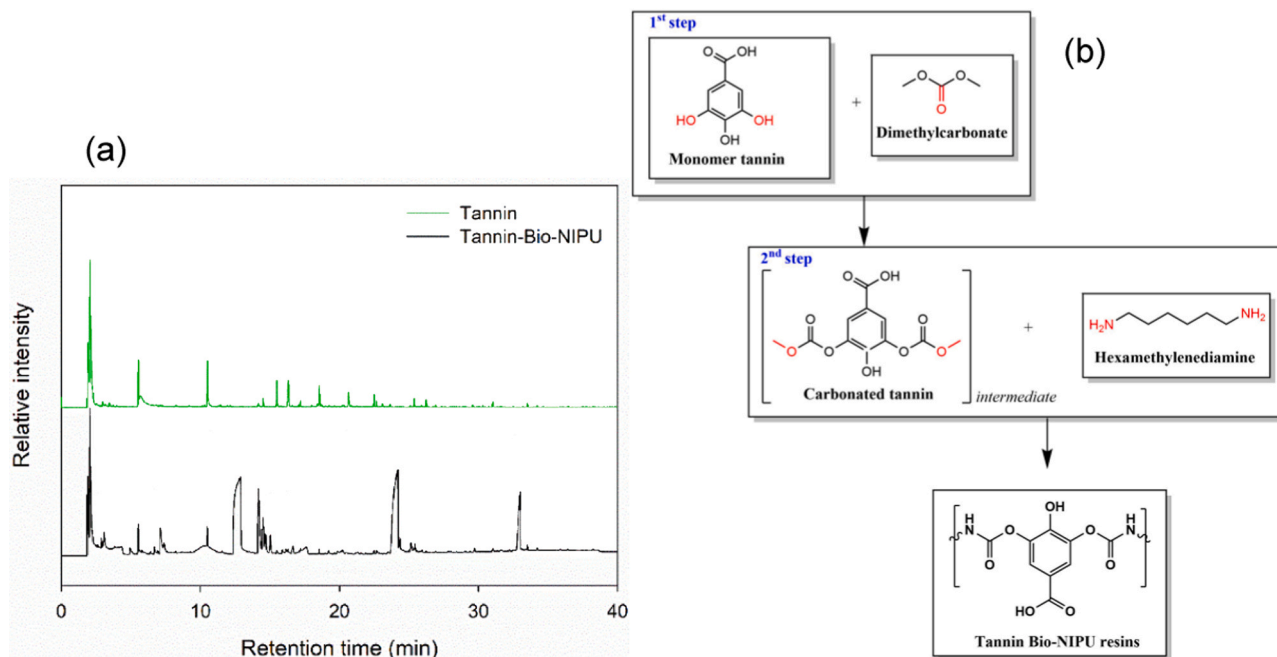


Fig. 5. Py-GCMS analysis of tannin-Bio-NIPU resins. (a) Pyrogram of tannin Bio-NIPU, (b) scheme reaction of tannin Bio-NIPU.

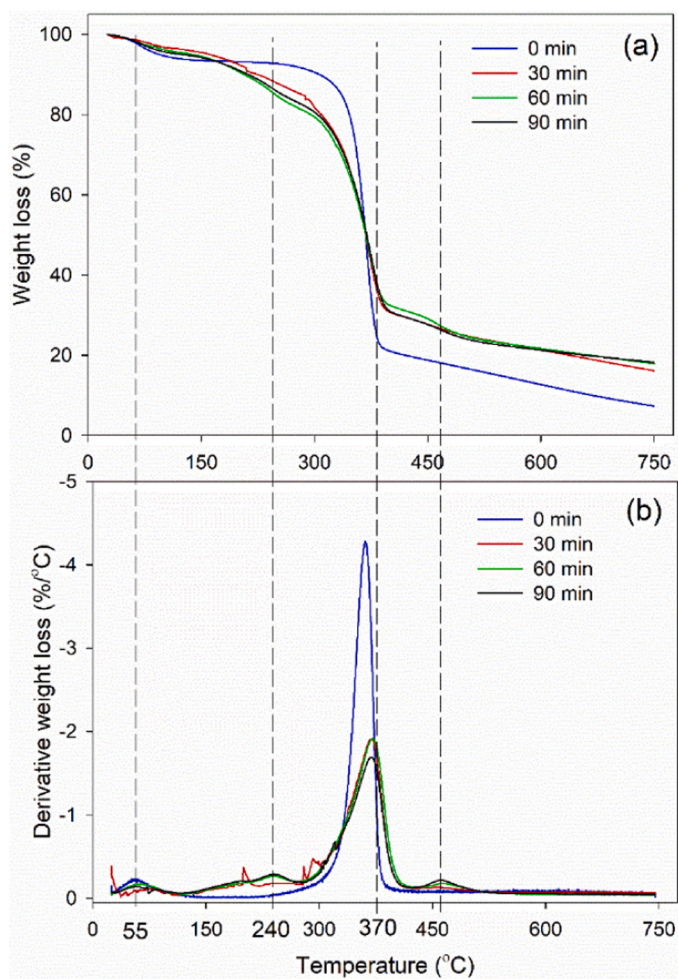


Fig. 6. Thermal stability of ramie fibers impregnated with tannin-Bio-NIPU resins for different times: (a) TGA, (b) DTG.

thermal stability of ramie fibers before impregnation (0 min) and after impregnation (30, 60, and 90 min) was determined. The first stage of losing water in fibers and the breakdown of parts with low molecular weights occurred at a temperature of 25–100 °C, resulting in a fairly minor reduction, around 5% (Fig. 6a) with a DTG of $\pm 0.01\%/^{\circ}\text{C}$ (Fig. 6b). When the temperature reached 240 °C, a 10% weight loss with a DTG of $\pm 0.02\%/^{\circ}\text{C}$ was determined for both types of samples. A significant difference was seen in the peak of DTG at $\pm 360\text{--}370^{\circ}\text{C}$ with a large average decrease of $\pm 1.8\text{--}4.3\%/^{\circ}\text{C}$ (Fig. 4b) and a weight loss of around 50–60% (Fig. 6a). TGA-DTG results at $\pm 360\text{--}370^{\circ}\text{C}$ showed that ramie fiber without impregnation experienced the highest degradation of around 60% with a DTG of $4.3\%/^{\circ}\text{C}$ compared to tannin-impregnated fiber made of Bio-NIPU resin, which only decreased and smaller DTG. When compared between the treatments of impregnation time used, the fiber showed less degradation as the impregnation time increases, indicating that the longer of impregnation time is applied, the greater the increase in the thermal stability of the resulting fiber.

A significant weight loss at temperatures above 300 °C was due to the degradation of the main chemical components of ramie fiber, i.e. lignin, cellulose, and hemicellulose. The cellulose glycosidic bonds break down at 300–400 °C, lignin starts to degrade at 280–500 °C, and the chemical component most easily broken down by heat occurs at 200–290 °C [33–35]. At a temperature of 360–750 °C, it was established that lignin with a high molecular weight was undergoing a process of decomposition [35–37]. The quantity of residue (char) left over after the heating process can also be used to determine the fiber's thermal stability; impregnated ramie fiber (0 min) has a char of $\pm 5\%$, impregnated ramie for 30 min is $\pm 18\%$, and for impregnated ramie with a time of 60 and 90 min shows a relatively similar char yield, which is around $\pm 24\text{--}25\%$. The thermal stability of ramie fibers was strongly influenced by the process and impregnation time, where impregnation times of 60 and 90 min provided better thermal stability than ramie without impregnation and ramie impregnated for 30 min. Because cross-links between the OH groups of the fiber and the urethane groups of the resin form during the impregnation process using tannin Bio-NIPU resin, ramie fibers' thermal stability may be increased [21,38].

The results obtained for the thermal and mechanical characteristics of ramie fibers before (0 min) and after impregnation (30, 60, and 90 min) can be seen in Fig. 7. The values of storage modulus (E') and loss

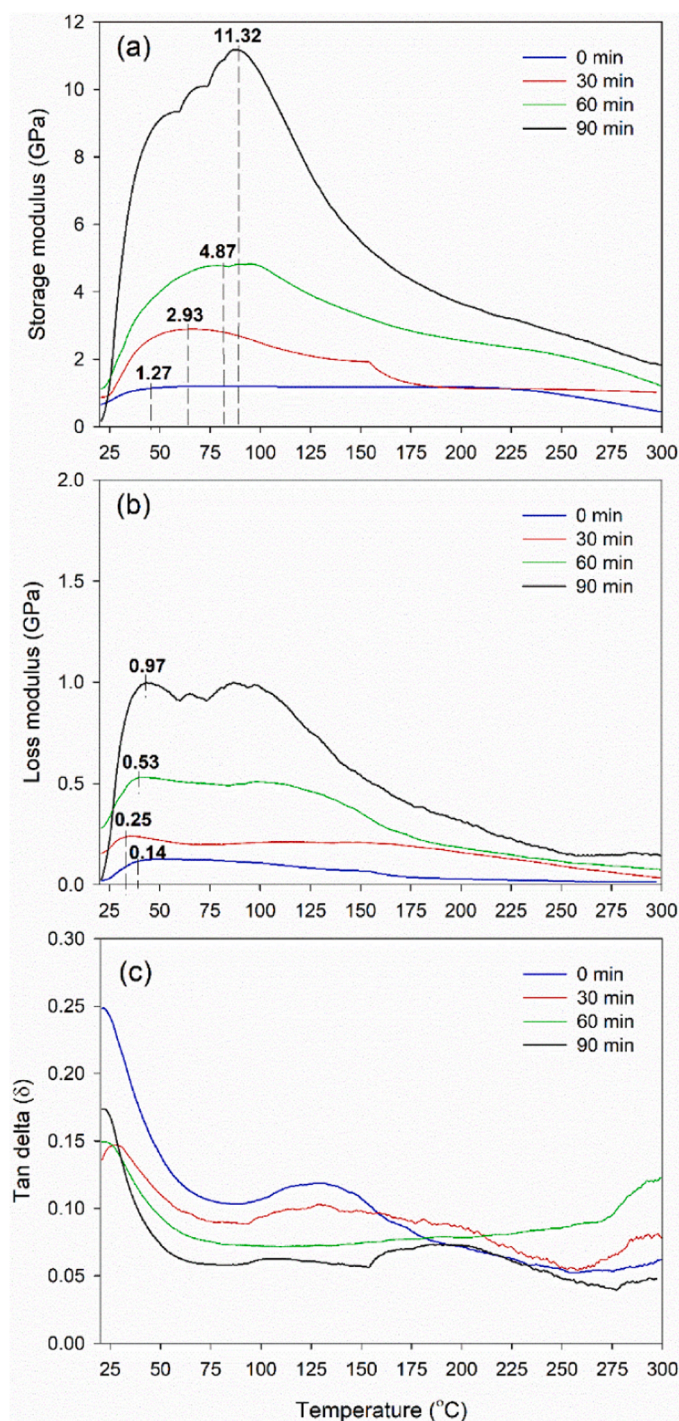


Fig. 7. Thermo-mechanical properties of ramie fibers impregnated with tannin-Bio-NIPU resins: (a) Storage modulus, (b) Loss modulus, (c) Tan delta.

modulus (E'') produced is directly proportional, where both values increase with increasing impregnation time applied. The impregnation process is proven to increase the E' and E'' values where the E' value of the fiber before impregnation was 1.27 GPa which then increased sequentially with the increase in impregnation time of 30, 60 and 90 min, namely 2.93, 4.87 and 11.32 GPa. Likewise, the value of E'' increased sequentially from 0, 30, 60, and 90 min, namely 0.14, 0.25, 0.53, and 0.97 GPa. Additionally, the temperature increase was associated with lower values.

Graphical representation of the thermo-mechanical properties of the ramie fibers impregnated with tannin Bio-NIPU resin is shown in Fig. 7.

The results of this thermomechanical value will increase the fiber's mechanical properties, which will be proportional to the results, with the impregnation process and along with the increase in the time the impregnation is applied. These two high values compared to the fibers before impregnation were caused by a strong bond between the OH groups of the fiber and the urethane resin groups, which caused the bond structure formed between the two to become tighter and more rigid, thus providing a hard segment to the impregnated fiber and indicated by an increase in the value storage modulus, besides that the impregnated fiber becomes more resistant to the movement of its molecular chains and improves its mechanical properties, so that the fiber does not break easily because the increase in value is positively correlated with sample hardness [27,39]. The resulting $\tan \delta$ value also confirmed the results of the storage and loss modulus values and showed inversely proportional results where the $\tan \delta$ value of non-impregnated fiber is higher than impregnated fiber (Fig. 7c).

3.5. Chemical component analysis of ramie fibers

The ramie fibers' pyrolysis results before (0 min) and after impregnation (30, 60, and 90 min) are shown in Fig. 8. There are several molecular fractions detected in the fibers before and after impregnation at various times such as Furfural, Butanal, 2-ethyl-, 4-Pentenoic acid, 4-methyl-, methyl ester, 2(5 H)-Furanone, and 1,2-Cyclopentanedione with varying abundance percentages up to 10%. The most visible differences were in the retention times of 15,09, 16,86, 26,36, and 34,62 min, which indicated the presence of a molecular fraction of 1,4-Dioxaspiro(2,4)heptan-5-one, 6-methyl-, 1,4:3,6-Dianhydro-.alpha.-d-glucopyranose, 1,3-Di-O-acetyl-.alpha.-.beta.-d ribopyranose, and 5-Aminovaleric acid, N-methoxycarbonyl-, methyl ester, which are only shown to exist in fiber impregnated fiber (30, 60, and 90 min) only while the fiber without impregnation (0 min) was unidentified, where the % relative abundance of each fraction increased as the impregnation time increased until it reached 33.77%. The fraction that appeared was due to the cross-linking between the OH groups of the ramie fiber and the NCO groups of the tannin Bio-NIPU resin used so that when it undergoes pyrolysis, it produces specific molecules which confirm that the impregnation process is going well. In addition, there was a molecular fraction characteristic of urethane cross-linking which was only shown in fibers impregnated for 90 min, namely the molecular fraction of Hexane, 1,6-diisocyanate- (5.16%) with a retention time of 21,09 min. Other molecular fractions that appeared only after 90 min of impregnation included 2-Cyclopenten-1-one, 3-methyl- (0.77%), 1 H-Pyrrole, 1-butyl- (0.27%), and Carbonic acid, monoamide, N -heptyl-, methyl ester (4.26%). Based on the pyrolysis results, the most optimum impregnation time is 90 min due to the confirmation of the number of bonds between ramie fibers and the tannin Bio-NIPU resin as indicated by the number of pyrolysis molecular fractions produced.

3.6. Surface morphology and chemical properties

FE-SEM EDX was used to compare the surface morphology and chemical characteristics of ramie fiber before and after impregnation. Fig. 8 shows ramie fibers before and after impregnation; there are morphological changes on the fiber surface. Fig. 9a shows that the non-impregnated ramie fibers (0 min) had a cleaner and smoother surface structure, and the fiber bundles still appeared to be completely separated from one another. It was different from impregnated fibers, whose contour characteristics were increasingly unclear, and the fiber bundles were increasingly unified as the impregnation time used was increased (Fig. 9b, c, and d). This is also one of the reasons why non-impregnated fibers tend to be finer and easier to decompose, while impregnated fibers are stiffer. The impregnation process also caused the darker colour of the fiber surface, and a layer of tannin Bio-NIPU resin, which was invisible in ramie fiber without impregnation, covered the fiber surface. It is evident that increasing the impregnation time used can cause the fiber

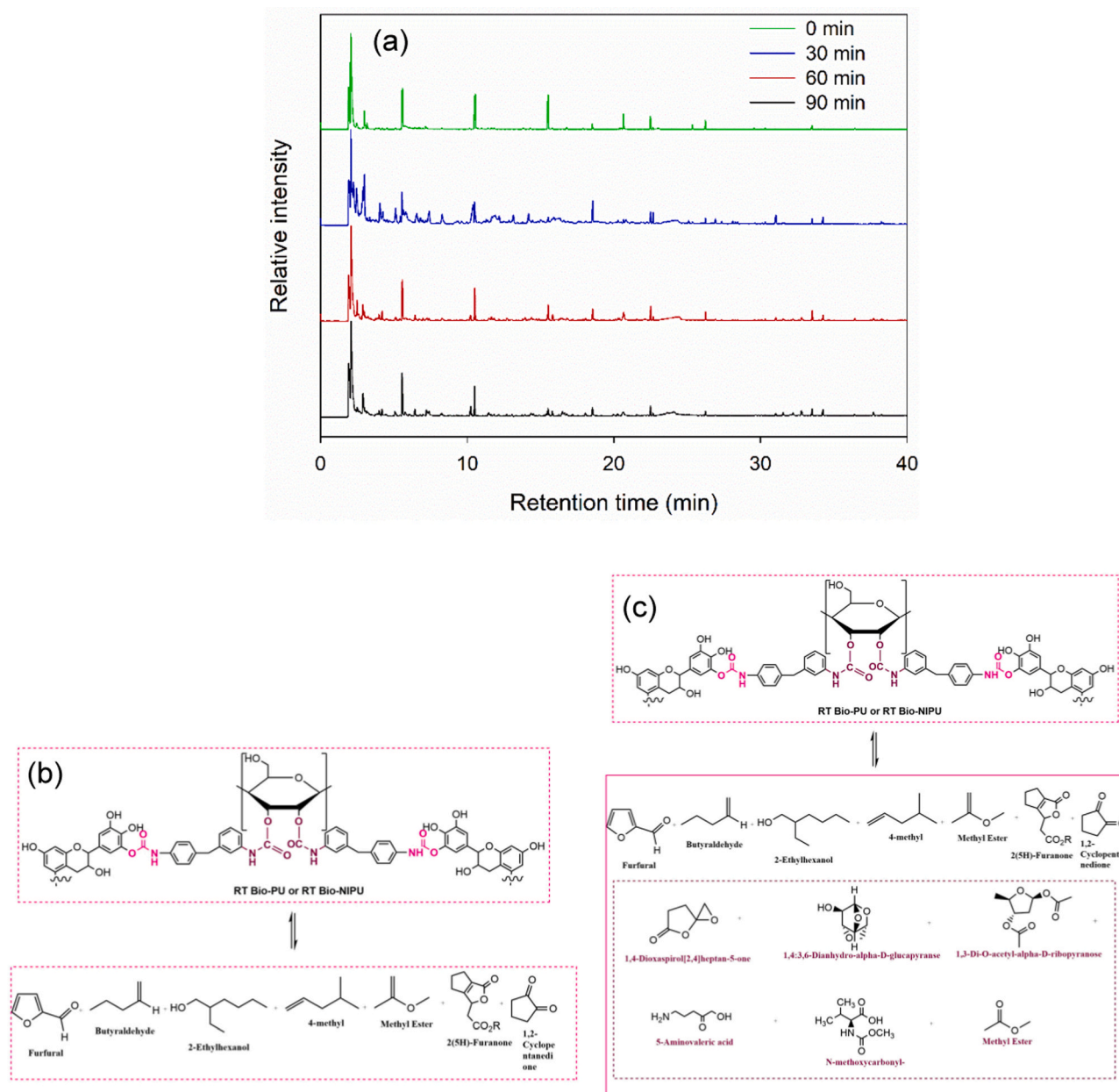


Fig. 8. Py-GCMS analysis of ramie fibers impregnated with tannin-Bio-NIPU resins for different times: (a) Pyrogram of natural and impregnated ramie fibers, (b) chemical species detected at natural ramie fibers after pyrolysis, (c) chemical species detected at impregnated ramie fibers after pyrolysis.

surface to be increasingly covered by resin because more resin seeps in and covers the fiber pores. Fig. 9d shows that the fiber bundles were fused, and their surface was covered by resin due to the long impregnation time used.

The EDX characterization was then used to conduct additional analysis pertaining to fiber particle elements, as shown in Fig. 10. Considering this figure, it is clear that carbon (53%) and hydrogen (47%) made up the majority of ramie fiber (0 min). A difference in the elemental content of the fiber was provided by the tannin Bio-NIPU resin impregnation process. Non-impregnated flax fiber contained 0% nitrogen, and impregnated (30, 60 and 90 min) contained an amount of elemental nitrogen varying from $\pm 2.4\%$ to $\pm 10\%$. The increase in the nitrogen content in ramie fiber was caused by the resin used, that contained urethane groups. Fig. 10 demonstrates the nitrogen content in impregnated ramie fiber increased with increasing time used, and 90 min of use had the highest nitrogen content, among others. The nitrogen content in the fiber impregnated with tannin bio-NIPU resin can

also be caused by using hexamethylenediamine, which contains several nitrogen groups in its structure and is used as a cross-linker in the formation of urethane bonds [40].

3.7. Mechanical properties of modified ramie fibers

The tensile strength and modulus of elasticity (MOE) tests were conducted on ramie fibers both prior to and subsequent to impregnation. The objective was to assess the impact of impregnation on the mechanical characteristics of the ramie fibers. A comparative analysis was undertaken to evaluate the data obtained from these tests. Fig. 11 present the tensile strength and MOE of the ramie fibers, respectively. The assessment of the tensile strength of ramie fibers holds significant relevance in the process of selecting ramie fibers for utilization as raw materials in the textile industry, thus necessitating its precise measurement [41,42]. The characteristic of a fiber to withstand a pre-determined level of longitudinal stress is commonly known as its tensile

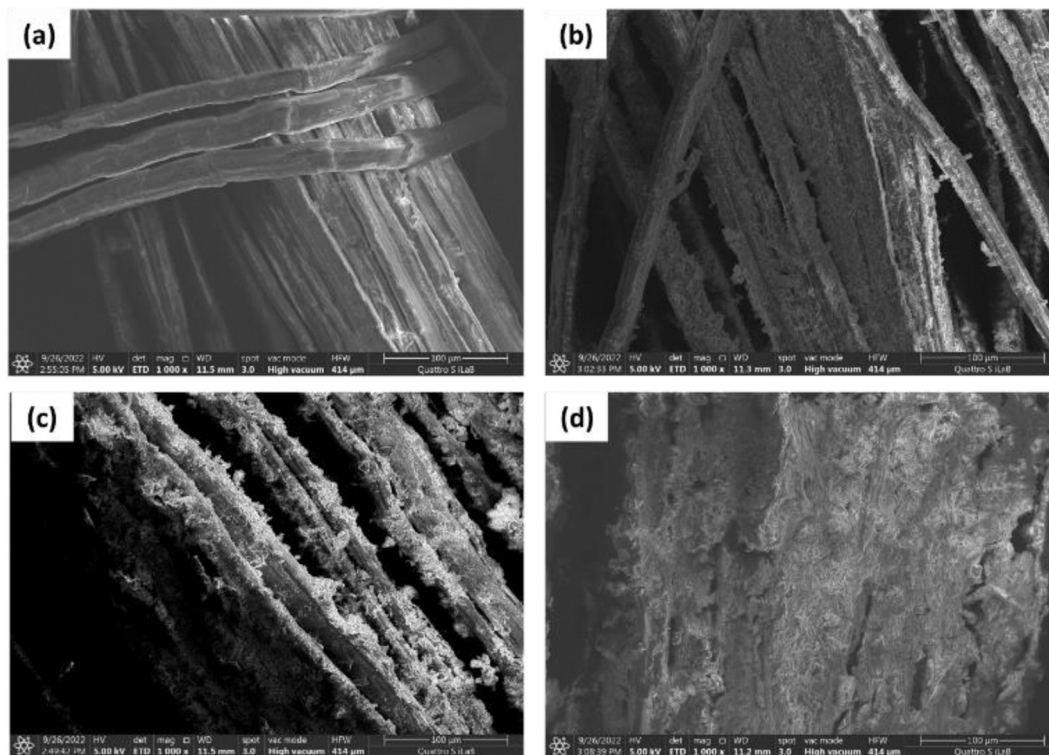


Fig. 9. FE-SEM images of impregnated ramie fibers with different times. (a) 0 min, (b) 30 min, (c) 60 min, (d) 90 min.

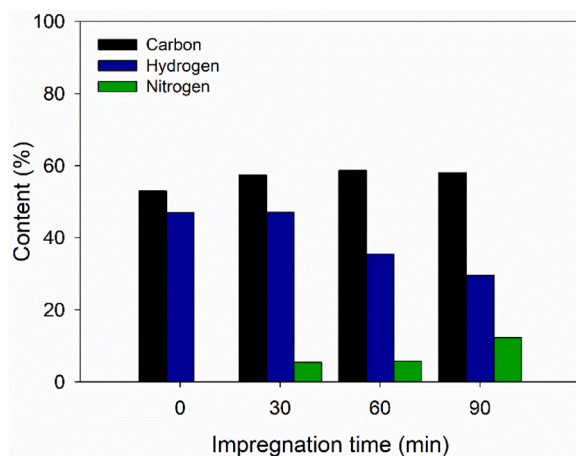


Fig. 10. EDX analysis of ramie fibers impregnated with tannin-Bio-NIPU resins for different times.

strength. In contrast to the post-impregnated fibers, the pre-impregnated fiber had the lowest tensile strength, measuring 267.57 MPa. On the contrary, the tensile strength of the ramie fibers exhibited an increase subsequent to its impregnation process, establishing its superiority as the most robust among the fibers subjected to post-impregnation. This is due to the formation of cross-links between the urethane groups of the resin and the hydroxyl groups in the hemp fiber which makes the tensile strength of the fiber after impregnation higher than before impregnation.

The results obtained from examining the tensile strength of ramie fibers after impregnation indicate an inverse relationship between the length of impregnation time and the resulting tensile strength of the fibers. The feasibility of this is achieved using fiber softening, which serves as a preliminary treatment for the ramie fiber being utilized. The increased smoothness of the fiber facilitates the achievement of this

outcome. However, the utilization of chemicals like hydrogen peroxide can cause harm to the chemical makeup of the fibers, resulting in a gradual reduction in its tensile strength. Besides chemical alteration, several other parameters can influence the mechanical properties of ramie fibers. These factors encompass the relative humidity of the surrounding environment, the microstructure, length, and diameter of the fiber [43,44]. Moreover, the moisture content of the fibers and the subsequent drying procedure can exert an influence on the mechanical characteristics of the fiber. The MOE values demonstrated an irregular pattern wherein the fibers prior to impregnation had a higher elastic modulus of 10.82 GPa compared to the respective MOE values of the fibers after impregnation, which ranged from 6.15 to 10.82 GPa (Fig. 11b). The low MOE value of the fiber after impregnation is caused by the more cross-links that form between the resin used and the hydroxyl groups in the hemp fiber, making the hemp fiber stiffer and its elasticity decreases, so that the MOE results are smaller than the fiber before impregnation.

4. Conclusions

Non-isocyanate polyurethane (NIPU) based on *Acacia mangium* tannin has been successfully synthesized in this study. The tannin bio-NIPU resin is thermally stable and rigid. When being used as impregnation for ramie fibers modification, it is demonstrated that the impregnation of ramie fibers with tannin bio-NIPU resin resulted in enhanced fiber characteristics. Markedly, the thermal stability of impregnated ramie fibers was strongly influenced by the impregnation time applied, where the impregnation times of 60 and 90 min provided better thermal stability compared to the ramie impregnated for 30 min. The optimal impregnation time was determined to be 90 min, as evidenced by its superior thermal stability with a residue of 25%. This impregnation time yielded the highest proportion of pyrolysis components and components exhibiting urethane cross-linking, as well as favorable thermal and mechanical properties compared to the other impregnation times used in this work. Additionally, it resulted in the most desirable

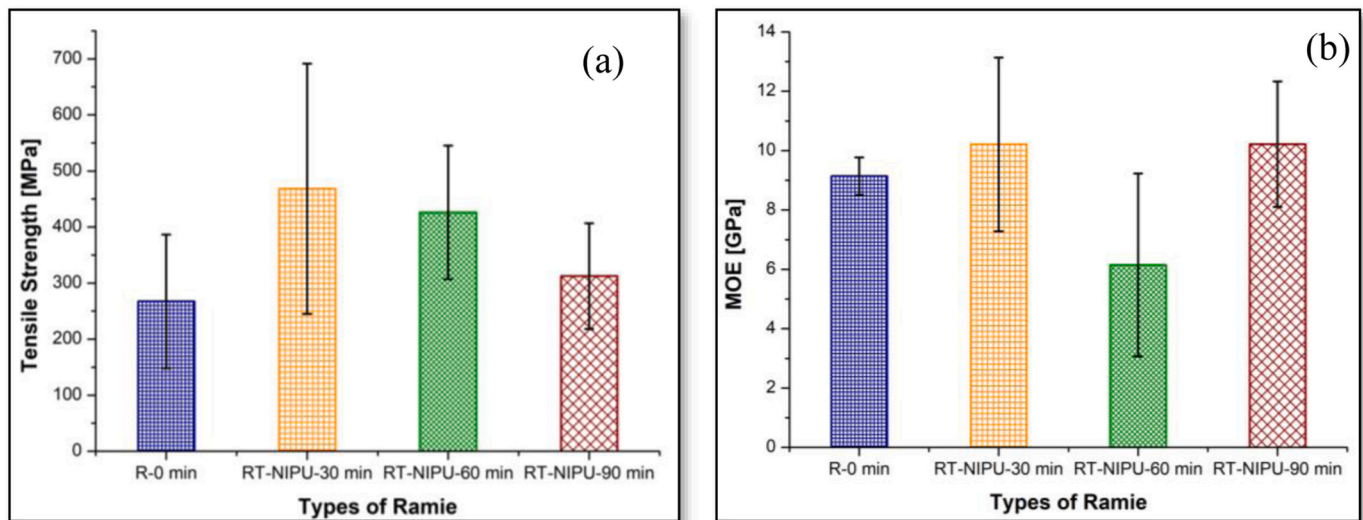


Fig. 11. Tensile strength (a) and MOE (b) of ramie fibers impregnated with tannin-Bio-NIPU resins at different times.

morphological properties. The observed disparities suggested that the resin achieved full penetration, together with the identification of the greatest concentration of nitrogen groups in the impregnated fiber after a duration of 90 min, indicating the presence of polyurethane. Based on the results obtained, it can be concluded that the impregnation of ramie fibers with a tannin-based NIPU represents a feasible technique for enhancing the thermal and mechanical properties of the fibers, thus increasing their potential applications as value-added functional materials.

The thermo-mechanical properties of natural fibers are critical for material design considerations, as well as processing and final material performance. It is typically critical for its applications in a variety of industry sectors. The improved thermo-mechanical properties of ramie fibers in this study could be beneficial for their applications in the automotive industry, as automotive components are frequently exposed to a wide range of temperatures. Fibers with superior thermo-mechanical properties are required to ensure the components' durability and performance. Furthermore, due to its non-toxic nature, tannin bio-NIPU resin could ensure a safe indoor car environment. Aside from that, ramie fibers with improved thermo-mechanical properties may find applications in the textile industry, where the fabrication of some protective clothing may necessitate materials with exceptional thermo-mechanical properties. Enhanced thermo-mechanical properties of fibers may also benefit a variety of industries, including construction, furniture, and packaging, where applications require greater thermal resistance and mechanical strength. Therefore, it can be concluded that the outcome of this study has a very promising application prospect and is worth continuous exploration.

Funding

This research and the APC was funded by World Class University from Universitas Sumatera Utara (USU), grant number 10/UN5.2.3.1/PPM/KP-WCU/2022 with a title "Pengembangan Perakat Poliuretan Ramah Lingkungan Non-Isosianat untuk Produk Panel Kayu".

Declaration of Competing Interest

The authors declare the following financial interests/personal relationships which may be considered as potential competing interests: Apri Heri Iswanto reports financial support was provided by University of Sumatera Utara.

Acknowledgements

The authors are grateful for the supports from integrated laboratory of bioproducts (iLaB), National Research and Innovation Agency of the Republic of Indonesia. This work was also supported by the RIIM Project titled "Teknologi Pengembangan Serat Rami Tahan Api Terimpregnasi Resin Poliuretan Sebagai Bahan Baku Tekstil Fungsional" led by Dr. Muhammad Adly Rahandi Lubis.

References

- [1] N.V. Gama, A. Ferreira, A. Barros-Timmons, Polyurethane foams: past, present, and future, *Materials* 11 (2018) 1–35, <https://doi.org/10.3390/ma11101841>.
- [2] M. Alinejad, S. Nikafshar, A. Gondaliya, S. Bagheri, N. Chen, S.K. Singh, D. B. Hodge, M. Nejad, Lignin-based polyurethanes: opportunities for and adhesives, *Polymers* 11 (2019) 1202.
- [3] M.A. Aristri, M.A.R. Lubis, S.M. Yadav, P. Antov, A.N. Papadopoulos, A. Pizzi, W. Fatriasari, M. Ismayati, A.H. Iswanto, Recent developments in lignin- and tannin-based non-isocyanate polyurethane resins for wood adhesives—a review, *Appl. Sci.* 11 (2021) 1–29, <https://doi.org/10.3390/app11094242>.
- [4] M. Thébault, A. Pizzi, S. Dumarçay, P. Gerardin, E. Fredon, L. Delmotte, Polyurethanes from hydrolysable tannins obtained without using isocyanates, *Ind. Crops Prod.* 59 (2014) 329–336, <https://doi.org/10.1016/j.indcrop.2014.05.036>.
- [5] M. Thébault, A. Pizzi, H.A. Essawy, A. Barhoum, G. Van Assche, Isocyanate free condensed tannin-based polyurethanes, *Eur. Polym. J.* 67 (2015) 513–526, <https://doi.org/10.1016/j.eurpolymj.2014.10.022>.
- [6] M. Thébault, A. Pizzi, F.J. Santiago-Medina, F.M. Al-Marzouki, S. Abdalla, Isocyanate-free polyurethanes by coreaction of condensed tannins with aminated tannins, *J. Renew. Mater.* 5 (2017) 21–29, <https://doi.org/10.7569/JRM.2016.634116>.
- [7] M. Pagliaro, L. Albanese, A. Scurrea, F. Zabini, F. Meneguzzo, R. Ciriminna, Tannin: a new insight into a key product for the bioeconomy in forest regions, *Biofuels Bioprod. Bioref.* 15 (2021) 973–979, <https://doi.org/10.1002/bbb.2217>.
- [8] [BPS] Badan Pusat Statistik, Statistics of forestry production, in: Direktorat Statistik Perikanan Perikanan dan Kehutanan (Ed.), Badan Pus. Stat., Badan Pusat Statistik, Jakarta (ID), 2023, 26.
- [9] R. Sukmawi, R. Sulaeman, E. Sribudiani, Pemanfaatan limbah kulit kayu Acacia mangium sebagai bahan baku papan partikel menggunakan perekat damar, *J. Ilmu-Ilmu Kehutan.* 4 (1) (2020) 6.
- [10] J. Merle, M. Birot, H. Deleuze, C. Mitterer, H. Carré, F.C.-E. Bouhtoury, New biobased foams from wood byproducts, *Mater. Des.* 91 (2016) 186–192, <https://doi.org/10.1016/j.matdes.2015.11.076>.
- [11] S. Mutiar, A. Kasim, A. Asben Emriadi, Quality of leather using vegetable tannins extract of Acacia mangium bark from waste of industrial plantation, *IOP Conf. Ser. Earth Environ. Sci.* 327 (2019) 1–7, <https://doi.org/10.1088/1755-1315/327/1/012012>.
- [12] X. Chen, X. Xi, A. Pizzi, E. Fredon, X. Zhou, J. Li, C. Gerardin, G. Du, Preparation and characterization of condensed tannin non-isocyanate polyurethane (NIPU) rigid foams by ambient temperature blowing, *Polymers* 12 (2020) 750, <https://doi.org/10.3390/polym12040750>.
- [13] X. Chen, A. Pizzi, X. Xi, X. Zhou, E. Fredon, C. Gerardin, Soy protein isolate non-isocyanates polyurethanes (NIPU) wood adhesives, *J. Renew. Mater.* 9 (2021) 1045–1057, <https://doi.org/10.32604/jrm.2021.015066>.

- [14] S. Basak, S.W. Ali, Sustainable fire retardancy of textiles using bio-macromolecules, *Polym. Degrad. Stab.* 133 (2016) 47–64, <https://doi.org/10.1016/j.polyimdegradstab.2016.07.019>.
- [15] Shahid-UI-Islam, B.S. Butola, *Advanced Textile Engineering Materials*, 2018. doi: 10.1002/9781119488101.
- [16] X. Chen, J. Li, X. Xi, A. Pizzi, X. Zhou, E. Fredon, G. Du, C. Gerardin, Condensed tannin-glucose-based NIPU bio-foams of improved fire retardancy, *Polym. Degrad. Stab.* 175 (2020) 109121, <https://doi.org/10.1016/j.polyimdegradstab.2020.109121>.
- [17] R. Erningsih, Cotton Knitting Fabric With Carbon Yarn Insertion, (2011).
- [18] M.A.R. Lubis, S.O. Handika, R.K. Sari, A.H. Iswanto, P. Antov, L. Kristak, L. Senghua, A. Pizzi, Modification of ramie fiber via impregnation with low viscosity bio-polyurethane resins derived from lignin, *Polymers* 14 (2022) 1–23, <https://doi.org/10.3390/polym14112165>.
- [19] Y.-Y. Wang, C.E. Wyman, C.M. Cai, A.J. Ragauskas, Lignin-based polyurethanes from unmodified kraft lignin fractionated by sequential precipitation, *ACS Appl. Polym. Mater.* 1 (2019) 1672–1679, <https://doi.org/10.1021/acsapm.9b00228>.
- [20] D.K. Chattopadhyay, D.C. Webster, Thermal stability and flame retardancy of polyurethanes, *Prog. Polym. Sci.* 34 (2009) 1068–1133, <https://doi.org/10.1016/j.progpolymsci.2009.06.002>.
- [21] S.O. Handika, M.A.R. Lubis, R.K. Sari, R.P.B. Laksana, P. Antov, V. Savov, M. Gajtanska, A.H. Iswanto, Enhancing thermal and mechanical properties of ramie fiber via impregnation by lignin-based polyurethane resin, *Materials* 14 (22) (2021) 1, <https://doi.org/10.3390/ma14226850>.
- [22] J. Lisperguer, Y. Saravia, E. Vergara, Structure and thermal behavior of tannins from *Acacia dealbata* bark and their reactivity toward formaldehyde, *J. Chil. Chem. Soc.* 61 (2016) 3188–3190, <https://doi.org/10.4067/S0717-97072016000400007>.
- [23] J. Gharib, S. Pang, D. Holland, Synthesis and characterisation of polyurethane made from pyrolysis bio-oil of pine wood, *Eur. Polym. J.* (2020) 109725, <https://doi.org/10.1016/j.eurpolymj.2020.109725>.
- [24] M. Amari, K. Khimeche, A. Hima, R. Chebout, A. Mezroua, Synthesis of green adhesive with tannin extracted from eucalyptus bark for potential use in wood composites, *J. Renew. Mater.* 9 (2021) 463–475, <https://doi.org/10.32604/jrm.2021.013680>.
- [25] N. Jesuarockiam, M. Jawaid, E.S. Zainudin, M.T. Hameed Sultan, R. Yahaya, Enhanced thermal and dynamic mechanical properties of synthetic/natural hybrid composites with graphene nanoplatelets, *Polymers* 11 (2019), <https://doi.org/10.3390/polym11071085>.
- [26] S.A.P. Sughantny, M.N.M. Ansari, A. Atiqah, Dynamic mechanical analysis of polyethylene terephthalate/hydroxyapatite biocomposites for tissue engineering applications, *J. Mater. Res. Technol.* 9 (2020) 2350–2356, <https://doi.org/10.1016/j.jmrt.2019.12.066>.
- [27] K. Selvakumar, O. Meenakshisundaram, Mechanical and dynamic mechanical analysis of jute and human hair-reinforced polymer composites, *Polym. Compos.* 40 (2019) 1132–1141, <https://doi.org/10.1002/pc.24818>.
- [28] L. He, F. Xia, Y. Wang, J. Yuan, D. Chen, J. Zheng, Mechanical and dynamic mechanical properties of the amino silicone oil emulsion modified ramie fiber reinforced composites, *Polymers* 13 (2021), <https://doi.org/10.3390/polym13234083>.
- [29] Y. Wang, X. Wang, Z. Ma, L. Shan, C. Zhang, Evaluation of the high-and low-temperature performance of asphalt mortar based on the DMA method, *Materials* 15 (2022) 1–12, <https://doi.org/10.3390/ma15093341>.
- [30] J.D. Menczel, R.B. Prime, *Thermal Analysis of Polymers: Fundamentals and Applications*, 2008. doi: 10.1002/9780470423837.
- [31] S. Basak, A.S.M. Raja, S. Saxena, P.G. Patil, Tannin based polyphenolic bio-macromolecules: creating a new era towards sustainable flame retardancy of polymers, *Polym. Degrad. Stab.* 189 (2021) 109603, <https://doi.org/10.1016/j.polyimdegradstab.2021.109603>.
- [32] M. Ismayati, A. Nakagawa-izumi, H. Ohi, Structural elucidation of condensed tannin from the bark waste of *Acacia crassicarpa* plantation wood in Indonesia, *J. Wood Sci.* 63 (2017) 350–359, <https://doi.org/10.1007/s10086-017-1633-4>.
- [33] F. Tomczak, K.G. Satyanarayana, T.H.D. Sydenstricker, Studies on lignocellulosic fibers of Brazil: part III - morphology and properties of Brazilian curauá fibers, *Compos. Part A Appl. Sci. Manuf.* 38 (2007) 2227–2236, <https://doi.org/10.1016/j.compositesa.2007.06.005>.
- [34] R. Kandimalla, S. Kalita, B. Choudhury, D. Devi, D. Kalita, K. Kalita, S. Dash, J. Kotoky, Fiber from ramie plant (*Boehmeria nivea*): a novel suture biomaterial, *Mater. Sci. Eng. C* 1 (2016) 1–2, <https://doi.org/10.1016/j.msec.2016.02.040>.
- [35] M.A. Aristri, R.K. Sari, M.A.R. Lubis, R.P.B. Laksana, P. Antov, A.H. Iswanto, E. Mardawati, S.H. Lee, V. Savov, L. Kristak, A.N. Papadopoulos, Eco-friendly tannin-based non-isocyanate polyurethane resins for the modification of Ramie (*Boehmeria nivea* L.) fibers, *Polymers* 15 (2023) 1492, <https://doi.org/10.3390/polym15061492>.
- [36] X. Xi, A. Pizzi, L. Delmotte, Isocyanate-free polyurethane coatings and adhesives from mono- and di-saccharides, *Polymers* 10 (2018) 1–21, <https://doi.org/10.3390/polym10040402>.
- [37] J. Saražin, A. Pizzi, S. Amirou, D. Schmiedl, M. Šernek, Organosolv lignin for non-isocyanate based polyurethanes (Nipu) as wood adhesive, *J. Renew. Mater.* 9 (2021) 881–907, <https://doi.org/10.32604/jrm.2021.015047>.
- [38] M.A. Aristri, M.A.R. Lubis, R.K. Sari, L. Kristak, A.H. Iswanto, E. Mardawati, L. S. Hua, Preparation and characterization of non-isocyanate polyurethane resins derived from tannin of *Acacia mangium* bark for the modification of ramie fibers, *Cent. Eur. For. J.* 69 (2023) 77–88, <https://doi.org/10.2478/forj-2023-0006>.
- [39] K. Naresh, K. Shankar, R. Velmurugan, Digital image processing and thermo-mechanical response of neat epoxy and different laminate orientations of fiber reinforced polymer composites for vibration isolation applications, *Int. J. Polym. Anal. Charact.* 23 (2018) 684–709, <https://doi.org/10.1080/1023666X.2018.1494431>.
- [40] T.T. Yang, J.P. Guan, R.C. Tang, G. Chen, Condensed tannin from *Dioscorea cirrhosa* tuber as an eco-friendly and durable flame retardant for silk textile, *Ind. Crops Prod.* 115 (2018) 16–25, <https://doi.org/10.1016/j.indcrop.2018.02.018>.
- [41] Z. Kan, M. bo Yang, W. Yang, Z. ying Liu, B. hu Xie, Investigation on the reactive processing of textile-ramie fiber reinforced anionic polyamide-6 composites, *Compos. Sci. Technol.* 110 (2015) 188–195, <https://doi.org/10.1016/j.compscitech.2015.01.023>.
- [42] M. Rehman, D. Gang, Q. Liu, Y. Chen, B. Wang, D. Peng, L. Liu, Ramie, a multipurpose crop: potential applications, constraints and improvement strategies, *Ind. Crops Prod.* 137 (2019) 300–307, <https://doi.org/10.1016/j.indcrop.2019.05.029>.
- [43] Z. Djafar, I. Renreng, M. Jannah, Tensile and bending strength analysis of ramie fiber and woven ramie reinforced epoxy composite, *J. Nat. Fibers* 0478 (2020), <https://doi.org/10.1080/15440478.2020.1726242>.
- [44] C.Z. Paiva Júnior, L.H. De Carvalho, V.M. Fonseca, S.N. Monteiro, J.R. M. D'Almeida, Analysis of the tensile strength of polyester/hybrid ramie-cotton fabric composites, *Polym. Test.* 23 (2004) 131–135, [https://doi.org/10.1016/S0142-9418\(03\)00071-0](https://doi.org/10.1016/S0142-9418(03)00071-0).